Silver deposition on titanium surface by electrochemical anodizing process reduces bacterial adhesion of *Streptococcus sanguinis* and *Lactobacillus salivarius*

Author

Maria Godoy-Gallardo [1,2], Ana G. Rodríguez-Hernández [3], Luis M. Delgado [1,2], José M. Manero [1,2], Francisco J. Gil [1, 2], Daniel Rodríguez [1, 2].

Affiliation

1 Biomaterials, Biomechanics and Tissue Engineering Group, Department of Materials Science and Metallurgical Engineering, Technical University of Catalonia (UPC-BarcelonaTECH), Barcelona, Spain.

2 Biomedical Research Networking Centre in Bioengineering, Biomaterials and Nanomedicine (CIBER-BBN), Zaragoza, Spain.

3Laboratory Biology of the Parasite Cytoskeleton, Department of Microbiology and Parasitology, Medical School, National Autonomous University of Mexico (UNAM), Mexico DF, Mexico.

Corresponding author: Maria Godoy Gallardo

ETSEIB-UPC - Department of Materials Science and Metallurgical Engineering

Av. Diagonal 647, 08028 - Barcelona, Spain.

Phone: +34 934054453

Fax: +34 934016706

maria.godoy.gallardo@upc.edu

Keywords: titanium, anodization, silver deposition, bacterial adhesion, antibacterial.

ABSTRACT

Objectives

The aim of this study was to determine the antibacterial properties of silver doped titanium surfaces prepared with a novel electrochemical anodizing process.

Material and Methods

Titanium samples were anodized with a pulsed process in a solution of silver nitrate and sodium thiosulphate at room temperature with stirring. Samples were processed with different electrolyte concentrations and treatment cycles to improve silver deposition. Physicochemical properties were determined by X-ray photoelectron spectroscopy, contact angle measurements, white-light interferometry and scanning electron microscopy. Cellular cytotoxicity in human fibroblasts was studied with Lactate Dehydrogenase assays. The *in vitro* effect of treated surfaces on two oral bacteria strains (*Streptococcus sanguinis* and *Lactobacillus salivarius*) was studied with viable bacterial adhesion measurements and growth curve assays. Non-parametric Kruskal-Wallis and U-Mann Whitney statistical tests were used for multiple and paired comparisons, respectively. *Post-hoc* Pearson correlation tests were calculated to check the dependence between bacteria adhesion and surface properties.

Results

X-ray photoelectron spectroscopy results confirmed the presence of silver on treated samples and showed that treatments with higher silver nitrate concentration and more cycles increased the silver deposition on titanium surface. No negative effects in fibroblast cell viability were detected and a significant reduction on bacterial adhesion *in vitro* was achieved in silver-treated samples compared to control titanium.

Conclusions

Silver deposition on titanium with a novel electrochemical anodizing process produced surfaces with significant antibacterial properties *in vitro* without negative effects on cell viability.

1. INTRODUCTION

Titanium and its alloys are widely used as biomaterials in many applications, such as dental implants, due to their excellent mechanical properties, biocompatibility and corrosion resistance *in vivo* (Aparicio et al. 2011; Williams 2001). Both biocompatibility and corrosion resistance are related to the strong affinity between titanium and oxygen, which results in the spontaneous formation of a surface oxide film when metal titanium is exposed to air (Bloyce A. et al. 1998; Oshida 2013).

Even though titanium has excellent properties for biomedical devices, titanium dental implants may fail due to biological factors, being peri-implantitis one of the most common (Pye et al. 2009). Peri-implantitis has been associated to dental plaque formation (Klinge et al. 2009; Fürst et al. 2007; Belibasakis 2013; Grössner-Schreiber et al. 2001). This oral biofilm starts with bacteria colonizing the implant surface. Early colonizers (such as *Streptococcus sanguinis*) play a key role on that process (Kolenbrander et al. 1990; Kilenbrander & London 1993; Hori & Matsumoto 2010), because they attach directly to the surface and guide the adhesion of later colonizers, such as *Porphyromonas gingivalis*, *Fusobacterium nucleatum* and *Aggregatibacter actinomycetemcomitans*, which have been associated directly to peri-implantitis (Kolenbrander & London 1993; Mayanagi et al. 2005). Other strains, as *Lactobacillus salivarius*, interacts with other colonizers and their by-products are essential for the biofilm formation and maintenance (Pham et al. 2009).

Peri-implantitis begins with an inflammation of the soft tissue around the implant (Montanaro et al. 2007; Arciola et al. 2011; Montanaro et al. 2011; Harris & Richards 2006) involving both epithelial structures and connective tissue elements (Berglundh et al. 1991; Artzi et al. 1993). Once a dental plaque matures on the exposed metallic surface, the degradation of the connective tissues may cause a loss of the biological seal. Thus, bacteria can migrate towards the apex of the implant and develop a new inflammation in the surrounding bone. If left untreated, it induces a progressive bone resorption, resulting in the dental implant failure (Klinge et al. 2005; Fürst et al. 2007; Artzi et al. 1993).

One of the most successful strategies to diminish the risk of peri-implantatis is to maintain the implant surfaces in contact with oral tissues as free as possible of bacteria (Klinge et al. 2005; Yoshinari et al. 2001; Zhao et al. 2009). Therefore, the incorporation of antibacterial compounds to titanium surfaces is a sound strategy to apply against peri-implantitis.

Silver and silver-base compounds are well-known antimicrobial agents, having a broad-spectrum activity against Gram-positive and Gram-negative bacteria, fungi, protozoa and certain viruses (Fox et al. 1969). The antimicrobial effect of the silver ion is well defined. Metallic silver, on the contrary, is relatively inert and poorly absorbed by bacteria. When in contact with wound fluids or other secretions, it ionizes and it is able to bind proteins and bacteria membranes (Atiyeh et al. 2007). The inhibitory action of silver is attributed to its interaction with structural proteins and it preferentially binds with DNA bases inhibiting bacteria replication (Yuan et al. 2013; Tamboli & Lee 2013; Radzig et al. 2013).

Different techniques have been explored to add silver onto biomaterial surfaces, such as ion implantation (Márquez et al. 2013; Wan et al. 2007; Li et al. 2007), physical vapor deposition (PVD) (Brook et al. 2007; Grodzicki et al. 2005) or production of a silver-containing hydroxyapatite coating attached to a titanium substrate by magnetron sputtering (Doo-Hoon Song 2011). These techniques, however, present some issues because their effectiveness are based on silver ion release, which markedly decreases from an initial upper value once in contact with physiological medium (Devasconcellos et al. 2012; Jamuna-Thevi et al. 2011). Besides, these processes are difficult to adapt to the manufacturing of medical devices with complex shapes, such as dental implants.

Anodization is a well-known electrochemical surface treatment technique that increases the width of the titanium oxide passive film. This oxide film acts as a barrier against the release of metallic ions, reducing surface reactivity and increasing corrosion resistance in the physiological medium (Gemelli & Camargo 2011). Already employed for color coding titanium dental implants and other prosthetic components (H.M. Kim et al. 1997; Sul et al. 2001), this process can be also used to modify the chemical composition of the surface adding new species. Deposition of silver onto titanium surfaces by anodization would be easily transferrable to industrial production of medical devices, as it is an easy and commonly employed technological procedure. Its use as a process for depositing silver on titanium has, however, some difficulties because of the positive charge of silver ion.

This work reports the development of a novel electrochemical anodizing process for adding silver on titanium surfaces, based on the use of a pulsed anodizing procedure to transfer a negatively charged silver coordinated complex onto the surface. The characteristics of the silver deposition were analyzed, as well as *in vitro* fibroblast viability, and the antibacterial properties were evaluated against S*treptococcus sanguinis* and *Lactobacillus salivarius*.

2. MATERIAL AND METHODS

2.1. Sample preparation and anodizing treatment

Commercially pure titanium grade II discs (10 mm diameter, 2 mm thickness) were cut from a stock rod, grinded with silicon carbide papers of decreasing grain size, and polished with a suspension of alumina particles (1.0 μm and 0.05 μm). Samples were sonicated in ethanol, distilled water and acetone for 15 minutes each, and dried with argon gas.

The samples were pre-treated in acid solution [250 mL HNO_3 60% (Panreac, Castellar del Vallès, Spain), 17.5 g NH_4HF_2 (Sigma-Aldrich, St.Louis, MO, USA) and 250 mL ultrapure distilled water (Millipore Milli-Q, Merck Millipore Corporation, Billerica, MA, USA)] for 10 seconds to remove surface contamination and the native surface titanium oxide layer (Vermesse et al. 2013).

The deposition of silver was done with an electrochemical anodizing process in aqueous solution with silver nitrate ($AgNO_3$) (Panreac) and a coordinating compound [sodium thiosulphate ($Na_2S_2O_3$)] (Panreac) at room temperature and with magnetic stirring. The complexation of silver follows the reaction (1):

$$Ag^+ + 2(S_2O_3)^{2-} \leftrightarrow [Ag(S_2O_3)_2]^{3-} \quad (1)$$

Titanium samples were used as a working electrode and a platinum sheet as counter electrode. The two main redox reactions expected at the anode are:

$$Ti \leftrightarrow Ti^{2+} + 2e^- \quad (2)$$

$$Ag^+ + e^- \leftrightarrow Ag \quad (3)$$

The anodizing process was controlled with a Potentiostat (PARSTAT 2273, Princeton Applied Research, Oak Ridge, TN, USA). A pulsed potential with a rectangular pulse shape (E_I = 0 V, E_F = 5 V, ST = 500 ms, SH = 10 mV, PW = 100 ms) was applied to the working electrode, with a full cycle period of 25 seconds (Fig. 1). After treatment, all samples were sonicated in ethanol, distilled water and acetone for 15 minutes each.

[Fig. 1]

A 2^2 experimental design with 4 process working conditions have been studied: two different electrolyte concentrations (concentration ratio $AgNO_3$:$Na_2S_2O_3$, concentration 1 (C1) = 0.1M:0.2M; concentration 2

(C2) = 0.05M:0.1M) and two treatment times (200 and 500 cycles). Samples were codified as C1_200, C1_500, C2_200 and C2_500, respectively. Non-treated titanium samples, coded as Ti, and samples anodized without $AgNO_3$ in the electrolyte, coded as NC1_500 and NC2_200, were used as control samples.

2.2. Physico-chemical characterization

2.2.1. Morphological analysis

Surface topography of the samples was observed with a Zeiss Neon40 Scanning Electron Microscope (SEM Carl Zeiss NTS GmbH, Jena, Germany). Images of uncoated samples were taken with secondary electrons at working distance of 7 mm and accelerating voltage of 5 kV. Three measurements were performed in three samples for each condition.

2.2.2. Roughness analysis

Surface roughness was measured with the optical profiling system WYKO NT1100 and WYKO Vision 232TM software (Veeco Instruments, Plainview, NY, USA) in vertical scanning interferometry (VSI) mode. The area analyzed was 736x480 µm for all samples. Three measurements were performed in three samples for each condition, computing three roughness parameters: arithmetic average height (R_a); skewness (R_{sk}, a measure of the symmetry of the profile about the mean line), and kurtosis (R_{ku}, a measure of the 'peakedness' of the profile) (Gademawla et al. 2002; Truong et al. 2010).

2.2.3. Contact angle analysis

Wettability of the samples was determined by static contact angle (CA) measurements of ultrapure distilled water with the sessile drop method (Contact Angle System OCA15 plus; Dataphysics, Filderstadt, Germany). The initial distilled water volume for each drop was 3 µL and all measurements were performed at 25ºC. Data was analyzed with SCA 20 software (Dataphysics) and three measurements were carried out for three different samples in each series.

2.2.4. Surface chemical characterization

Titanium surfaces were analyzed by X-ray photoelectron spectroscopy (XPS) with an Mg anode XR50 source operating at 150 W and a Phoibos 150 MCD-9 detector (D8 advance, SPECS Surface Nano Analysis GmbH, Berlin, Germany). Spectra were recorded with pass energy of 25 eV at 0.1 eV steps at a pressure below $7.5 \cdot 10^{-9}$ mbar. Binding energies were referred to the C 1s signal at 284.8 eV.

Three samples were studied for each working condition. The ratios silver/titanium and sulfur/titanium were calculated from the measured elemental surface composition.

2.3. Biological characterization

2.3.1. *In vitro* cell viability of human fibroblasts

Human foreskin fibroblasts (HFFs, Merck Millipore Corporation, Billerica, MA, USA) were cultured in Dulbecco's Modified Eagle Medium (DMEM) supplemented with 10% (v/v) fetal bovine serum (FBS), 1% (w/v) L-glutamine, 1% penicillin/streptomycin (50 U/mL and 50 µg/mL) (all reagents from Invitrogen, Carlsbad, CA, USA) at 37ºC in a humidified incubator and 5% (v/v) CO_2, renewed every 2 days. Cells passage eight was used in all experiments.

Confluent HFFs were detached from the culture flask by incubation with TrypLE (Invitrogen) for 5 min. The HFFs solution was centrifuged at 300g for 5 min and re-suspended in new culture medium. Cells were then seeded onto titanium samples with a density of 5000 cells/disc and incubated at 37ºC. After 4 hours, 1, 3 and 7 days of incubation, cells were lysed with 200 µL/well of M-PER® (Pierce, Rockford, IL, USA). The *in vitro* cell viability of cultured HFFs on the studied surfaces was determined with the Cytotoxicity Detection Kit LDH (Roche Applied Science, Mannheim, Switzerland). The absorbance for each sample was read at 490 nm with an ELx800 Universal Microplate Reader (Bio-Tek Instruments, Inc. Winooski, VT, USA). Tissue culture polystyrene (TCPS) samples were used as positive controls and three measurements were carried out for three different samples in each series.

2.3.2. Bacterial assays

Bacterial assays were done with two oral bacterial strains: *Streptococcus sanguinis* (CECT 480, Colección Española de Cultivos Tipo (CECT), Valencia, Spain) and *Lactobacillus salivarius* (CCUG 17826, Culture Collection University of Göteborg (CCUG), Göteborg, Sweden). *S. sanguinis* was growth and maintained in Todd-Hewitt (TH) broth (Scharlau Todd-Hewitt broth, Scharlab SL, Sentmenat, Spain) and *L. salivarius* in MRS broth (Scharlau MRS broth, Scharlab SL).

Cultures were incubated overnight at 37ºC before each assay. The optical density of each bacterial suspension was adjusted to 0.2 ± 0.01 at 600 nm, giving approximately $1 \cdot 10^8$ colony forming units (CFU)/mL for each strain.

2.3.2.1. Bacterial adhesion assay

Samples were immersed in 1 mL of bacterial suspension ($1 \cdot 10^8$ CFU/mL) for 2 hours at 37ºC. After this time, the medium was suctioned and samples washed twice with PBS (Gibco, Paisley, UK). Adherent bacteria were detached by vortexing the discs for 5 minutes in 1 mL of PBS. Detached bacteria were then seeded using serial dilutions on TH agar plates (Scharlau agar, Scharlab SL) for *S. sanguinis* and MRS agar plates (Scharlau agar, Scharlab SL) for *L. salivarius*. The plates were then incubated at 37ºC for 24 h and the resulting colonies counted. Alternatively, for slow growing colonies the plates were incubated for an extra 24 h period, and the number of bacterial colonies counted again. Three samples for each condition were studied and two different dilution of each sample were seeded in two different agar plates.

2.3.2.2. Bacterial growth curve assay

Samples were immersed in 1 mL of diluted bacterial suspension ($1 \cdot 10^2$ CFU/mL) for 24 hours. Bacterial growth was monitored every hour during the first 8 hours, and at 24 hours. To determine the number of bacteria at the specified time points, 25 µL-aliquots were extracted from the bacterial suspensions and mixed with 75 µL of medium. The absorbance of these mixtures was measured at 600 nm using a multimode microplate reader (Infinite 200 PRO, Tecan, Männedorf, Switzerland) and three measurements were performed for each condition.

2.4. Statistical analysis

Non-parametric U Mann-Whitney statistical tests were used to analyze differences in contact angle, cell viability and proliferation and bacterial adhesion between treated and control surfaces. Non-parametric Kruskal-Wallis statistical tests were used to analyze differences in the ratios of surface chemical composition. *Post-hoc* Pearson correlation was calculated to check the dependence between bacteria adhesion and silver presence. Significance level was set at a P value<0.05.

3. RESULTS

3.1. Physico-chemical characterization

3.1.1. Morphological analysis

As shown in Fig. 2a, control titanium samples (Ti) displayed a smooth surface with some minor polishing scratches due to sample preparation. SEM images showed a topographical effect of the anodization process on all treated samples with the shape of rounded etching (Fig. 2 (b-g)). Silver-anodized titanium samples, besides, had on their surface deposits with globular morphology (arrows in Fig. 2 (d-g)). Examination of the treated surfaces showed that these deposits were homogeneously dispersed on the whole titanium surface and remained attached to the surfaces, even after sonication of the samples (ethanol, distilled water and acetone for 15 minutes each).

[Fig. 2]

3.1.2. Roughness analysis

Values of the roughness parameters R_a, R_{ku} and R_{sk} are shown in table 1. Mean surface roughness changed after anodizing when compared to control (Ti). The R_a measures for C1_200 and NC1_500 were the highest and the increment was almost three times compared to control titanium mean roughness. For the scanned areas, R_{ku} showed the highest measurements in samples treated at 500 cycles (C1_500 and C2_500), followed for surfaces treated with 200 cycles (C1_200 and C2_200); whereas controls (NC1_500, NC2_200 and Ti) presented the lower values and did not show any significant differences among them. For R_{sk} results, all samples showed values higher than zero, and there were no significant differences between treated and control samples.

[Table 1]

3.1.3. Contact angle analysis

Variations in wettability were measured in the samples using the sessile drop method (Fig. 3). NC1_500 and NC2_200 presented the lowest contact angle values. Silver-anodized titanium samples (C1_500, C1_200, C2_500 and C2_200) have a slightly increased wettability compared to control treated samples. Throughout the process of anodization, the changes observed were statistically significant between silver-treated samples (C1_500, C1_200 and C2_500) and control treated samples (NC1_500 and NC2_200) according to U Mann-Whitney statistical analysis.

[Fig. 3]

3.1.4. Surface chemical characterization

Quantitative elemental composition of the XPS survey spectra, as well as relative concentration ratio of silver and sulfur to titanium ([Ag]/[Ti] and [S]/[Ti] ratios), are shown in table 2.

[Table 2]

Silver-anodized titanium samples (C1_200, C1_500, C2_200 and C2_500) characteristically had silver (1.1% for C1_200, 2.8% for C1_500, 1% for C2_200 and 0.5% for C2_500) and sulfur (0.6% for C1_200, 1.5% for C1_500, 0.5% for C2_200 and 0.5% for C2_500) on the surface, as well as reduction on the percentage of oxygen and titanium, compared to control titanium (Ti). Control treated samples (NC1_500 and NC2_200), however, did not show a measurable presence of silver or sulfur, but had an increment in carbon and a decrement in oxygen and titanium compared to Ti.

The [Ag]/[Ti] ratios did not show a statistical correlation with neither concentration nor number of cycles for anodizing. Samples treated with the lowest silver concentration (C2) presented the same [Ag]/[Ti] ratio, irrespective of the number of cycles, whilst sample anodized with the highest silver concentration for 500 cycles (C1_500) had the highest [Ag]/[Ti] ratio.

[Fig. 4]

Fig. 4 shows high resolution Ag 3d, Ti 2p and O 1s XPS peaks for C1_500 surfaces. The Ag 3d high resolution spectra consisted in three peaks related to metallic (Ag:369 eV) and oxide states (AgO:367 eV, Ag_2O: 367.8 eV) according to previous reports (Ferraria et al. 2012; McCormick et al. 2002; Gao et al. 2004). The binding energy of Ag $3d^5/_2$ was 367 eV, whereas for Ag $3d^3/_2$ the binding energy was 373 eV, with a difference of 6 eV between both peaks.

The Ti 2p high resolution spectra, with the electron level Ti $2p^3/_2$ at 458 eV and the Ti 2p½ at 464 eV, was deconvoluted in three peaks originating from the metallic (Ti) and oxide states (TiO_2 and TiO) (López et al. 2011; Kang et al. 2009). The difference between peaks was 5.66 eV. The O 1s high resolution spectra were deconvoluted in oxide peaks near 530 eV, OH^- bound at 532 eV and chemisorbed water molecules peaks near 533 eV.

[Table 3]

The concentration of Ag 3d was quantified after deconvolution for all samples (table 3). Titanium samples anodized for 500 cycles showed, for each concentration, an increase in metallic silver compared to samples treated for 200 cycles.

3.2. Biological characterization

3.2.1. Cell viability - Lactate Dehydrogenase (LDH) assay

Cell viability behavior was similar for all samples within the studied time frame (Fig. 5). After 4 hours of culture, silver-anodized surfaces showed a slightly minor number of viable cells than the other surfaces; after 1 day of incubation, the samples maintained similar values, with a small increment at 3 days of incubation. Differences were statistically significant among treated samples and control samples for each time (indicated with a line in the plot), but lower than 10% in all cases.

[Fig. 5]

3.2.2. Bacterial assay

3.2.2.1. Bacterial adhesion assay

Results of bacterial adhesion assays of both *S. sanguinis* and *L. salivarius* strains on titanium surfaces after 2 hours of incubation are shown in table 4. Control treated samples (NC1_500 and NC2_200) presented higher bacterial adhesion amount than other surfaces and closer to titanium control (Ti) for both strains. Titanium anodized with silver for 500 cycles (C1_500 and C2_500) presented lower bacteria count than surfaces treated with silver for 200 cycles (C1_200 and C2_200). The lowest amount of attached bacteria was measured for the sample C1_500 for both strains. Changes were statistically significant between silver-treated samples (C1_500, C1_200, C1_200 and C2_500) and titanium control samples according to U Mann-Whitney statistical analysis.

[Table 4]

3.2.2.2. Bacterial growth curve assay

Bacteria growth curves showed a differentiated response of each strain to the surface treatment during bacteria growth. *S. sanguinis* (Fig. 6a) presented a stable value for the initial 6 hours of culture. Bacteria growth curve for *L.salivarius* (Fig. 6b), however, presented a slight decrease in the first part of the curve (2 hours) for all treated samples. Afterwards, all titanium samples presented almost the same absorbance

value among them but lower than bacteria medium. After 9 hours of incubation, the amount of bacteria started to decrease on all treated surfaces for both strains.

[Fig. 6]

4. DISCUSSION

In this study, silver has been deposited on titanium surface by means of an electrochemical anodizing process with complexated silver. Silver is a widely used biocide, with similar effects that antibiotics but without the resistance that bacteria develop against them (Zhao et al. 2009; J. Kim et al. 2008). The use of silver as antimicrobial agent before development of a biofilm can be effective to prevent the bacteria adhesion on treated surfaces, as previously demonstrated by Hori *et al* (Hori & Matsumoto 2010). However, once the biofilm is formed, the effectiveness of antimicrobial agents is greatly reduced (Silvestry-Rodriguez et al. 2008; Dufour et al. 2010). An effective strategy on medical devices requires, therefore, that the biomaterial surface presents a null or highly reduced bacteria attachment to the surface.

Improvements in the development of silver deposition techniques are thoroughly researched. Some progresses are based on Ag^+ ion release (Márquez et al. 2013; Wanet al. 2007; Li et al. 2007; Brook et al. 2007; Doo-Hoon Song 2011) but silver use in that state suffers a decrease in its concentration over time. On the other hand, other procedures apply silver to surfaces with antibacterial effects induced when combined with UV, visible light irradiation (J.Y.Kim et al. 2008; Ashkarran et al. 2011) or in combination with other substances such as calcium phosphates (Melo et al. 2013). The method developed in the present study to deposit silver on titanium surfaces has a very low release of silver into the medium. Moreover, the antibacterial effect of silver-anodized surfaces does not require the application of external agents, such as UV irradiation. The electrochemical process presented in this study deposits silver on titanium surface (C1_500, C1_200, C2_500 and C2_200) as shown by XPS (table 2). Deconvolution of the high resolution spectra (Fig. 4) revealed peaks at energy positions corresponding to silver oxide (AgO: 367eV, Ag_2O: 367.8eV) and metallic silver (Ag: 369eV) (Ferraria et al. 2012; McCormick et al. 2002; Gao et al. 2004; Boronin et al. 1998; Wang et al. 1998), demonstrating its presence on treated samples. In addition, it was observed that for the same number of cycles but using a higher electrolyte concentration, a higher ratio [Ag]/[Ti] was measured. An increment on the number of cycles had also an effect on the ratio [Ag]/[Ti] for C1 concentration, but not for C2 concentration (table 2). These results suggest that silver deposition depends more on silver concentration in the electrolyte than on the number

of cycles applied, in agreement to published results on electrochemical processing of silver nanoparticles by Liu *et al* (Liu et al. 2013) and Yin *et al* (Yin et al. 2014).

Possible cytotoxic effects of treated surfaces were studied with LDH cell viability assays. These tests revealed a slight reduction in the number of viable cells, quantified at 7 days about 10% lower than TCPS control sample. When silver is incorporated and fixed into a substrate, the toxicity of the deposition might be due to direct contact with the seeded cells. Data on potential in vivo toxic effects on silver are limited. According to a study of *Necula et al* (Necula et al. 2012), there is a cytotoxic level of Ag^{+}, but histological analysis by *Marsich et al* (Marsich et al. 2013) demonstrated no cytotoxic effect of silver on bone tissue for concentrations with antibacterial effects. In the present study, the minor reduction in cell viability indicates a low or non-cytotoxic effect due to the silver deposition, as stated in the standard ISO 10993-5.

In general, it is described that bacterial colonization is enhanced on rough surfaces because of surface features, such as valleys, depressions, pits and edges (Hecht & Strehblow 1997; Wu et al. 2011; Rodríguez-Hernández et al. 2013; Zhu

et al. 2004. Montanaro *et al* (Montanaro et al. 2007) and Amoroso *et al* (Amoroso et al. 2006) postulated that a surface roughness below 200 nm did not enhance the bacteria adhesion because the size of surface irregularities was not large enough to offer increased bacterial retention. In this study, results showed that pre-treated samples presented a roughness value lower than 100 nm, and it could be considered lower than the cut-off value and suggested that it will not influence in bacterial adhesion. Moreover, skewness parameter measurements were close to zero, with a equal distribution between peaks and valleys (Gadelmawla et al. 2002; Fuss 2011) and kurtosis showed values greater than 3, being a distribution curve with few high peaks and low valleys (Gadelmawla et al. 2002).

In addition to roughness parameters, wettability was also analyzed. It has been described that decreased contact angle enhanced the interaction between implant surfaces and the biological environment (Dexter 1979; Baier et al. 1968; Baier et al. 1984), influencing cells and bacteria adhesion (Rodríguez-Hernández et al. 2013; Amoroso et al. 2006; Dexter 1979). Following the results presented in Fig. 3, it is obvious that the contact angle values measured for the silver-treated surfaces versus the control titanium surface do not present a significant difference. Hence, within the scope of this study, changes in bacteria adhesion to silver-treated surfaces compared to control surfaces can not be attributed to changes in surface wettability.

The results presented in Fig. 7 evidence that the surface with the highest amount of deposited silver (C1_500) presented the lowest surface density of bacteria, especially *S.sanguinis* (table 4), while surfaces of the control group (NC1_500, NC2_200 and Ti) had the highest amount of attached bacteria. These results confirm the effectiveness of silver anodizing against *in vitro* bacteria adhesion to treated titanium surfaces. As a precursor of biofilm formation, any reduction in the *S. sanguinis* adherence to dental implant surfaces will reduce or delay dental plaque formation and the possibility of peri-implantitis (Grössner-Schreiber et al. 2001; Kolenbrander et al. 1990). A decrease on the *L. salivarius* attachment would also hinder the development of the oral biofilm, because of its role in dental plaque maintenance (Pham et al. 2009).

[Fig. 7]

A *post-hoc* statistical test was performed in order to evaluate possible relationships between surface properties and bacteria adherence onto surfaces. Bacteria adhesion for *S. sanguinis* and *L. salivarius* strains is plotted versus roughness and contact angle in Fig. 7. The Spearman correlation of bacteria adhesion with roughness (Fig. 7a and 7b) is 0.00 for *S. sanguinis* (P = 1) and -0.036 for *L. salivarius* (P = 0.939). In the case of contact angle, Spearman correlation is -0.107 for *S. sanguinis* (P = 0.819) and -0.143 for *L. salivarius* (P = 0.760). These P values indicate a lack of statistically significant correlation between the reduction in CFU/mm^2 and variations in both parameters. However, when was plotted the adhesion bacteria from *S. sanguinis* and *L. salivarius* in control samples (NC1_500, NC2_200 and Ti) *versus* contact angle (Fig. 7c and 7d), a correlation between wettability and amount of adhered bacteria was observed. A lower number of attached bacteria for lower contact angle surfaces was determined, specially for *S. sanguinis*, in accordance to Amoroso *et al* results (Amoroso et al. 2006).

Furthermore, the relationship between the amount of adhered bacteria and the [Ag]/[Ti] ratio was analysed too (Fig. 7e and 7f). Spearman correlation of bacteria adhesion with the ratio [Ag]/[Ti] is -0.898 for *S.sanguinis* (P = 0.006) and -0.898 for *L.salivarius* (P = 0.006). This result indicates a correlation between an increased deposition of silver on titanium surfaces and a decrease in bacterial adhesion to the silver-treated surfaces.

Bacterial studies also showed the effect of the surface modification on the early (up to 6 hours) planktonic bacteria growth curves. Particularly, *S. sanguinis* growth curve had a delay at the first part of the curve with the immersed sample C1_500. However, *L. salivarius* has not such a change. These results suggest

that silver may not be released into the medium at the minimum inhibitory rate necessary for reducing the growth of planktonic bacteria. It also indicates that the antibacterial effects are constrained to bacteria in contact with the treated surface, as shown by the decrease of adhered bacteria on silver-anodized titanium samples.

These positive results lead to consider the study of complementary processes for increasing the amount of silver on the treated surfaces, as well as the *in vivo* effectiveness of silver anodization against bacteria biofilms in future works.

5. CONCLUSIONS

A novel electrochemical anodizing process for depositing silver on titanium surfaces has been developed. Silver was deposited in metallic and oxidized state on the titanium surface. The roughness of the treated surfaces increased, but the wettability was maintained when compared to untreated titanium.

Titanium surfaces treated with this process presented a significant decrease on *in vitro* bacterial adhesion for the bacterial strains *S. sanguinis* and *L. salivarius*, diminishing the risk of biofilm formation. The bacterial adhesion reduction was statistically correlated to the concentration of silver on the treated surfaces. Moreover, all treated samples showed good *in vitro* biocompatibility.

A titanium surface treated with this anodization process is expected not only to have a good biocompatibility but also antibacterial properties, with a potential application in dental implants.

ACKNOWLEDGEMENTS

This investigation was supported by the Research Grant MAT2009-12547 from the Ministry of Science and Innovation (MICINN). The authors also express their gratitude to Dr. Virginia Paredes, for her useful comments and advices regarding the XPS analysis.

REFERENCES

Amoroso, P.F., Adams, R.J., Waters, M.G.J. & Williams, D.W. (2006) Titanium surface modification and its effect on the adherence of Porphyromonas gingivalis: an in vitro study. *Clinical Oral Implants Research* **17**: 633-637.

Aparicio, C., Padrós, A. & Gil, F-J. (2011) In vivo evaluation of micro-rough and bioactive titanium dental implants using histometry and pull-out tests. *Journal of the Mechanical Behavior of Biomedical Materials* **4**: 1672-1682.

Arciola, C.R., Visai, L., Testoni, F., Arciola, S., Campoccia, D., Speziale P. & Montanaro, L. (2011) Concise survey of Staphylococcus aureus virulence factors that promote adhesion and damage to peri-implant tissues. *The International Journal of Artificial Organs* **34**: 771-780.

Artzi, Z., Tal, H., Moses, O. & Kozlovsky, A. (1993) Mucosal considerations for osseointegrated implants. *The Journal of Prosthetic Dentistry* **70**: 427-432.

Ashkarran, A.A., Aghigh, S.M., Kavianipour, M. & Farahani, N.J. (2011) Visible light photo-and bioactivity of Ag/TiO2 nanocomposite with various silver contents. *Current Applied Physics* **11**: 1048-1055.

Atiyeh, B.S., Costagliola, M., Hayek, S.N. & Dibo, S.A. (2007) Effect of silver on burn wound infection control and healing: review of the literature. *Burns: Journal of the International Society for Burn Injuries* **33**: 139-148.

Baier, R.E., Shafrin, E.G. & Zisman, W.A. (1968) Adhesion: mechanisms that assist or impede it. *Science* **162**: 1360-1368.

Baier, R.E., Meyer, A.E., Natiella, J.R. & Carter, J.M. (1984) Surface properties determine bioadhesive outcomes: Methods and results. *Journal of Biomedical Materials Research* **18**: 337-355.

Belobasakis, G.N. (2013) Microbiological and immuno-pathological aspects of peri-implant diseases. *Archives of Oral Biolog.y*

Berglundh, T., Lindhe, J., Ericsson, I., Marinello, C.P., Liljenberg, B. & Thomsen, P. (1991) The soft tissue barrier at implants and teeth. *Clinical Oral Implants Research* **2**: 81-90.

Bloyce, A., Qi, P.Y., Dong, H. & Bell, T. (1998) Surface modification of titanium alloys for combined improvements in corrosion and wear resistance. *Surface and Coatings Technology* **107**: 125-132.

Boronin, A., Koscheev, S. & Zhidomirov, G. (1998) XPS and UPS study of oxygen states on silver. *Journal of Electron Spectroscopy and Related Phenomena* **96**: 43-51.

Brook, L.A., Evans, P., Foster, H.A., Pemble, M.E., Steele, A., Sheel, D.W. & Yates, H.M. (2007) Highly bioactive silver and silver/titania composite films grown by chemical vapour deposition. *Journal of Photochemistry and Photobiology A: Chemistry* **187**: 53-63.

Williams, D.F.(2001) Titanium for medical applications. In: Brunette, D.M., Tengvall, P., Textor, M. & Thomsen, P. (2001) Titanium in Medicine: Material Science, Surface Science, Engineering, Biological Responses, and Medical Applications. p.13. Springer.

Devasconcellos, P., Bose, S., Beyenal, H., Bandyopadhyay, A. & Zirkle, L.G. (2012) Antimicrobial particulate silver coatings on stainless steel implants for fracture management. *Materials Science and Engineering: C* **32**: 1112-1120.

Dexter, S.C. (1979) Influence of substratum critical surface tension on bacterial adhesion—in Situ studies. *Journal of Colloid and Interface Science* **70:** 346-354.

Doo-Hoon S. & Soo-Hyuk, U. Antimicrobial silver-containing titanium oxide nanocomposite coatings by a reactive magnetron sputtering. *Thin Solid Films* **519**: 7079-7085.

Dufour, D., Leung, V. & Lévesque, C.M. (2010) Bacterial biofilm: structure, function, and antimicrobial resistance. *Endodontic Topics* **22**: 2-16.

Ferraria, A.M., Carapeto & Botelho do Rego, A.M. (2012) X-ray photoelectron spectroscopy: Silver salts revisited. *Vacuum* **86**: 1988-1991.

Fox, C.L.Jr., Rappole, B.W. & Stanford, W. (1969) Control of pseudomonas infection in burns by silver sulfadiazine. *Surgery, Gynecology & Obstetrics* **128**: 1021-1026.

Fürst, M.M., Salvi, G.E., Lang, N.P. & Persson, G.R. (2007) Bacterial colonization immediately after installation on oral titanium implants. *Clinical Oral Implants Research* **18**: 501-508.

Fuss, F.K. (2011) The effect of surface skewness on the super/postcritical coefficient of drag of roughened cylinders. *Procedia Engineering* **13**: 284-289.

Gadelmawla, E.S., Koura, M.M., Maksoud, T.M.A., Elewa, I.M. & Soliman, H.H. (2002) Roughness parameters. *Journal of Materials Processing Technology* **123**: 133-145.

Gao, X-Y., Wang, S-Y., Li, J., Zheng, Y-X., Zhang, R-J., Zhou, P., Yang, Y-M. & Chen, L-Y. (2004) Study of structure and optical properties of silver oxide films by ellipsometry, XRD and XPS methods. *Thin Solid Films* **455**: 438-442.

Gemelli, E. & Camargo, N.H.A. (2011) Low voltage anodization of titanium in nitric acid solution: A new method to bioactivate titanium. *Materials Characterization* **62**: 938-942.

Grodzicki, A., Lakomska, I., Piszcek, P., Szymańska, I. & Szlyk, E. (2005) Copper(I), silver(I) and gold(I) carboxylate complexes as precursors in chemical vapour deposition of thin metallic films. *Coordination Chemistry Reviews* **249**: 2232-2258.

Grössner-Schreiber, B., Griepentrog, M., Haustein, I., Müller, W.D., Lange, K.P., Briedigkeit, H. & Göbel, U.B. (2001) Plaque formation on surface modified dental implants. *Clinical Oral Implants Research* **12**: 543-551.

Harris, L.G. & Richards, R.G. (2006) Staphylococci and implant surfaces: a review. *Injury* **37**: S3-14.

Hecht, D. & Strehblow, H-H. (1997) XPS investigations of the electrochemical double layer on silver in alkaline chloride solutions *Journal of Electroanalytical Chemistry* **440**: 211-217.

Hori, K. & Matsumoto, S. Bacterial adhesion: From mechanism to control. *Biochemical Engineering Journal* **48**: 424-434.

Jamuna-Thevi, K., Bakar, S.A., Ibrahim, S., Shahab, N. & Toff, M.R.M. (2011) Quantification of silver ion release, in vitro cytotoxicity and antibacterial properties of nanostuctured Ag doped TiO2 coatings on stainless steel deposited by RF magnetron sputtering. *Vacuum* **86**: 235-241.

Kang, B-S., Sul, Y-T., Oh, S-J., Lee, H-J. & Albrektsson, T. (2009) XPS, AES and SEM analysis of recent dental implants. *Acta Biomaterialia* **5**: 2222-2229.

Kim, H.M., Miyaji, F., Kokubo, T. & Nakamura, T. (1997) Effect of heat treatment on apatite-forming ability of Ti metal induced by alkali treatment. *Journal of Materials Science: Materials in Medicine* **8**: 341-347.

Kim, J., Pitts, B., Stewart, P.S., Camper, A. & Yoon, J. (2008) Comparison of the Antimicrobial Effects of Chlorine, Silver Ion, and Tobramycin on Biofilm. *Antimicrobial Agents and Chemotherapy* **52**: 1446-1453.

Kim, J.Y., Lee, C., Cho, M. & Yoon, J. Enhanced inactivation of E. coli and MS-2 phage by silver ions combined with UV-A and visible light irradiation. *Water Research* **42**: 356-362.

Klinge, B., Hultin, M. & Berglundh, T. (2005) Peri-implantitis. *Dental Clinics of North America* **49**:661-676.

Kolenbrander, P.E., Andersen, R.N. & Moore, L.V. Intrageneric coaggregation among strains of human oral bacteria: potential role in primary colonization of the tooth surface. *Applied and Environmental Microbiology* **56**: 3890-3894.

Kolenbrander, P.E. & London, J. (1993) Adhere today, here tomorrow: oral bacterial adherence. *Journal of Bacteriology* **175**: 3247-3252.

Li, J.X., Wang, J., Shen, L.R., Xu, Z.J., Li, P., Wan, G.J. & Huang, N. (2007) The influence of polyethylene terephthalate surfaces modified by silver ion implantation on bacterial adhesion behavior. *Surface and Coatings Technology* **201**: 8155-8159.

Liu, Y., Rosenfield, E., Hu, M. & Mi, B. Direct observation of bacterial deposition on and detachment from nanocomposite membranes embedded with silver nanoparticles. *Water Research* **47**: 2949-2958.

López, M.F., Jiménez, J.A. & Gutiérrez, A. (2011) XPS characterization of surface modified titanium alloys for use as biomaterials. *Vacuum* **85**: 1076-1079.

Márquez, H., Salazar, D., Rangel-Rojo, R., Angel-Valenzuela, J.L., Vázquez, G.V., Flores-Romero, E., Rodríguez-Fernández, L. & Olver, A. (2013) Synthesis of optical waveguides in SiO2 by silver ion implantation. *Optical Materials* **35**: 927-934.

Marsich, E., Travan, A., Donati, I., Turco, G., Kulkova, J., Moritz, N., Aro, H.T., Crosera, M. & Paoletti, S. (2013) Biological responses of silver-coated thermosets: An in vitro and in vivo study. *Acta Biomaterialia* **9**: 5088-5099.

Mayanagi, G., Sato, T., Shimauchi, H. & Takahashi, N. (2005) Microflora profiling of subgingival and supragingival plaque of healthy and periodontitis subjects by nested PCR. *International Congress Series* **1284**: 195-196.

McCormick, H., McMillan, R., Merrett, K., Bensebaa, F., Deslandes, Y., Dubé, M. & Sheardown, H. (2002) XPS study of the effect of the conditions of peptide chemisorption to gold and silver coated polymer surfaces. *Colloids and Surfaces B: Biointerfaces* **26**: 351-363.

Melo, M.A.S., Cheng, L., Zhang, K., Weir, M.D., Rodriguez, L.K.A. & Xu, H.H.K. (2013) Novel dental adhesives containing nanoparticles of silver and amorphous calcium phosphate. *Dental Materials* **29**: 199-210.

Montanaro, L., Campoccia, D. & Arciola, C.R. (2007) Advancements in molecular epidemiology of implant infections and future perspectives. *Biomaterials* **28**: 5155-5168.

Montanaro, L., Testoni, F., Poggi, A., Visai, L., Speziale, P. & Arciola, C.R. (2011) Emerging pathogenetic mechanisms of the implant-related osteomyelitis by Staphylococcus aureus. *The International Journal of Artificial Organs* **34**: 781-788.

Necula, B.S., Van Leeuwen, J.P.T.M., Fratila-Apachitei, L.E., Zaat, S.A.J, Apachitei, I. & Duszczyk, J. In vitro cytotoxicity evaluation of porous TiO2–Ag antibacterial coatings for human fetal osteoblasts. *Acta Biomaterialia* **8**: 4191-4197.

Oshida, Y. (2013) 4 - Oxidation and Oxides. In: Bioscience and Bioengineering of Titanium Materials, 2nd edition, p. 87-115. Oxford: Elsevier.

Pham, L.C., Van Spanning, R.J.M., Röling, W.F.M., Prosperi, A.C., Terefework, Z., Ten Cate, J.M., Crielaard, W. & Zaura, E. (2009) Effects of Probiotic Lactobacillus Salivarius W24 on the Compositional Stability of Oral Microbial Communities. *Archives of Oral Biology* **54**: 132-137.

Pye, A.D., Lockhart, D.E.A., Dawson, M.P., Murray, C.A. & Smith, A.J. A Review of Dental Implants and Infection. *The Journal of Hospital Infection* **72**: 104-110.

Radzig, M.A., Nadtochenko, V.A., Koksharova, O.A., Kiwi, J., Lipasova, V.A. & Khmel, I.A. (2013) Antibacterial effects of silver nanoparticles on gram-negative bacteria: Influence on the growth and biofilms formation, mechanisms of action». *Colloids and Surfaces B: Biointerfaces* **102**: 300-306.

Rodríguez-Hernández, A.G., Muñoz-Tabares, J.A., Godoy-Gallardo, M., Juárez, A. & Gil, J-F. S. sanguinis adhesion on rough titanium surfaces: Effect of culture media». *Materials Science and Engineering: C* **33**: 714-720.

Silvestry-Rodriguez, N., Bright, K.R., Slack, D.C., Uhlmann, D.R. & Gerba, C.P. (2008) Silver as a Residual Disinfectant To Prevent Biofilm Formation in Water Distribution Systems. *Applied and Environmental Microbiology* **74**: 1639-1641.

Sul, Y-T., Johansson, C.B., Jeong, Y. & Albrektsson, T. The electrochemical oxide growth behaviour on titanium in acid and alkaline electrolytes». *Medical Engineering & Physics* **23**: 329-346.

Tamboli, D.P. & Lee, D.S. (2013) Mechanistic antimicrobial approach of extracellularly synthesized silver nanoparticles against gram positive and gram negative bacteria». *Journal of Hazardous Materials* **260**: 878-884.

Truong, V.K., Lapovok, R., Estrin, Y.S., Rundell, S., Wang, J.Y., Fluke, C.J., Crawford, R.J. & Ivanova, E.P. (2010) The Influence of Nano-Scale Surface Roughness on Bacterial Adhesion to Ultrafine-Grained Titanium. *Biomaterials* **31**: 3674-3683.

Vermesse, E., Mabru, C. & Arurault, L.(2013) Surface integrity after pickling and anodization of Ti–6Al–4V titanium alloy». *Applied Surface Science* **285**: 629-637.

Wan, Y.Z., Raman, S., He, F. & Huang, Y. Surface modification of medical metals by ion implantation of silver and copper. *Vacuum* **81**: 1114-1118.

Wang, J-H., Dai, W-L-, Deng, J-F., Wei, X-M., Cao, Y-M. & Zhai, R-S. (1998) Interaction of oxygen with silver surface at high temperature». *Applied Surface Science* **126**: 148-152.

Wu, Y., Zitelli, J.P., TenHuisen, K.S., Yu, X. & Libera, M.R. Differential Response of Staphylococci and Osteoblasts to Varying Titanium Surface Roughness. *Biomaterials* **32**: 951-960.

Yin, T., Walker, H.W., Chen, D. & Yang, Q. Influence of pH and ionic strength on the deposition of silver nanoparticles on microfiltration membranes». *Journal of Membrane Science* **449**: 9-14.

Yoshinari, M., Oda, Y., Kato, T. & Okuda, K. (2001) Influence of surface modifications to titanium on antibacterial activity in vitro. *Biomaterials* **22**: 2043-2048.

Yuan, Z., Li, J., Xu, B., Zhang, H. & Yu, C-P. (2013) Interaction of silver nanoparticles with pure nitrifying bacteria». *Chemosphere* **90**: 1404-1411.

Zhao, L., Chi, P.K., Zhang, Y. & Wu, Z. (2009) Antibacterial Coatings on Titanium Implants. *Journal of Biomedical Materials Research Part B: Applied Biomaterials* **91B**: 470-480.

Zhu, X., Chen, J., Schaideler, L., Reichl, R. & Geis-Gerstorfer, J. (2004) Effects of Topography and Composition of Titanium Surface Oxides on Osteoblast Responses. *Biomaterials* **25**: 4087-4103.

Table 1. Roughness parameters for the each treatment [mean ± standard deviation], median and IQR. ([a]): statistically significant difference versus control sample (Ti). (P value < 0.05).

	R_a (nm)	median	IQR	R_{ku} (nm)	median	IQR	R_{sk} (nm)	median	IQR
C1_200	91 ± 9[a]	91.3	15.8	9 ± 4	8.7	4.6	1.2 ± 0.6[a]	1.2	1.1
C1_500	76 ± 7[a]	79.9	13.2	11 ± 6	9.4	5.0	1.0 ± 0.8[a]	0.9	1.1
C2_200	80 ± 21[a]	79.6	44.4	9 ± 4	8.2	6.7	0.2 ± 0.8[a]	0.2	1.1
C2_500	67 ± 10[a]	67.3	10.3	16 ± 12	13.9	12.5	0.7 ± 1.0[a]	0.7	1.8
NC1_500	89 ± 8[a]	84.5	13.8	7 ± 4	5.4	6.6	0.4 ± 0.9[a]	0.5	1.0
NC2_200	81 ± 16[a]	79.1	25.5	8 ± 3	7.5	4.4	0.4 ± 0.4[a]	0.5	0.7
Ti	31 ± 9	28.9	12.2	6 ± 3	4.2	5.4	0.3 ± 0.1	0.3	0.2

Table 2. Surface chemical composition determined by XPS analysis [mean ± standard deviation], median and IQR. (*): Measurement below detection limit. ([a]):Statistically significant difference among the ratio [Ag]/[Ti] of treated samples was determined by Kruskal-Wallis. (0,015, P value < 0.05).

	C 1s	N 1s	O 1s	S 2p	Ti 2p	Ag 3d
C1_200	37.2 ± 3.1	1.4 ± 1	50.3 ± 0.3	0.6 ± 0.2	9.4 ± 5.1	1.1 ± 0.4
C1_500	46.0 ± 9.7	1.0 ± 0.4	42.9 ± 5.3	1.5 ± 0.6	5.8 ± 4.2	2.8 ± 0.9
C2_200	36.3 ± 3.5	1.2 ± 0.4	51.5 ± 1.7	0.5 ± 0.1	9.7 ± 5.5	1.0 ± 0.1
C2_500	48.7 ± 4.4	2.8 ± 0.3	41.9 ± 4.8	0.5 ± 0.1	5.8 ± 0.7	0.5 ± 0.1
NC1_500	61.2 ± 0.6	1.1 ± 0.7	35.4 ± 0.3	*	1.8 ± 0.2	*
NC2_200	50.7 ± 0.8	3.4 ± 0.5	42.0 ± 1.4	*	4.3 ± 1.2	*
Ti	24.3 ± 0.3	1.1 ± 1.0	57.7 ± 0.3	*	16.8 ± 1.2	*

	[Ag]/[Ti]	median	IQR	[S]/[Ti]	median	IQR
C1_200	0.2 ± 0.01 [a]	0.2	0.2	0.09 ± 0.05	0.1	0.1
C1_500	0.6 ± 0.3 [a]	0.6	0.4	0.3 ± 0.1	0.3	0.2
C2_200	0.1 ± 0.06 [a]	0.1	0.1	0.06 ± 0.04	0.1	0.1
C2_500	0.1 ± 0.03 [a]	0.1	0.1	0.06 ± 0.02	0.1	0.1
NC1_500				0.2 ± 0.01	0.2	0.2
NC2_200						
Ti						

Table 3. Energy bindings and concentration (%) from the XPS analysis treated surfaces [mean ± standard deviation], median and IQR.

3 d5/2					
	Bond state	**Position (eV)**	**At % Ag**	**median %**	**IQR**
C1_200	AgO	366.8 ± 0.8	4.6 ± 1.5	4.1	1.0
	Ag_2O	367.9 ± 0.2	85.6 ± 3.4	86.8	2.4
	Ag	368.8± 0.4	9.8 ± 2.0	9.1	1.4
C1_500	AgO	367.2 ± 0.1	7.3 ± 1.4	6.8	1.0
	Ag_2O	367.82 ± 0.3	80.6 ± 2.0	79.9	1.4
	Ag	368.6 ± 0.2	12.2 ± 3.4	13.4	2.4
C2_200	AgO	366.8 ± 0.4	5.4 ± 2.3	4.6	1.6
	Ag_2O	367.9 ± 0.3	85.4 ± 2.0	86.0	1.4
	Ag	368.8 ± 0.3	9.1 ± 0.3	9.3	0.2
C2_500	AgO	367.1 ± 0.2	8.0 ± 0.5	7.8	0.4
	Ag_2O	367.6 ± 0.1	77.9 ± 2.7	77.0	1.9
	Ag	368.2 ± 0.3	14.0 ± 3.3	15.2	2.3

Table 4. Adhesion of *S. sanguinis* and *L. salivarius* after 2 hours of incubation at 37ºC [mean ± standard deviation], median and IQR. ([a]) ([b]): statistically significant difference compared to control sample (Ti). (P value < 0.05).

Sample	*S. sanguinis* [CFU/mm^2]	median	IQR	*L. salivarius* [CFU/mm^2]	median	IQR
C1_200	$3.8\cdot10^3 \pm 4.4\cdot10^{2a}$	8073.7	1357.1	$8.1\cdot10^3 \pm 1\cdot10^{3b}$	3824.4	825.0
C1_500	$2.4\cdot10^2 \pm 4.0\cdot10^{1a}$	5218.2	703.7	$5.2\cdot10^3 \pm 4\cdot10^{2b}$	2321.7	743.1
C2_200	$4.1\cdot10^3 \pm 5.1\cdot10^{2a}$	8370.7	1550.1	$8.3\cdot10^3 \pm 8.\cdot10^{2b}$	4178.1	961.3
C2_500	$3.2\cdot10^2 \pm 4.1\cdot10^{1a}$	7400.2	1575.9	$7.3\cdot10^3 \pm 8.4\cdot10^{2b}$	3276.8	788.2
NC1_500	$6.4\cdot10^3 \pm 8.\cdot10^2$	12507.0	1563.2	$1.2\cdot10^4 \pm 9\cdot10^3$	6695.4	1402.7
NC2_200	$6.2\cdot10^3 \pm 3.2\cdot10^2$	13188.7	4717.6	$1.2\cdot10^4 \pm 2.6\cdot10^3$	6151.0	610.0
Ti	$8.0\cdot10^3 \pm 1\cdot10^3$	13534.2	3083.5	$1.4\cdot10^4 \pm 1.7\cdot10^3$	8356.1	1814.0

Figures

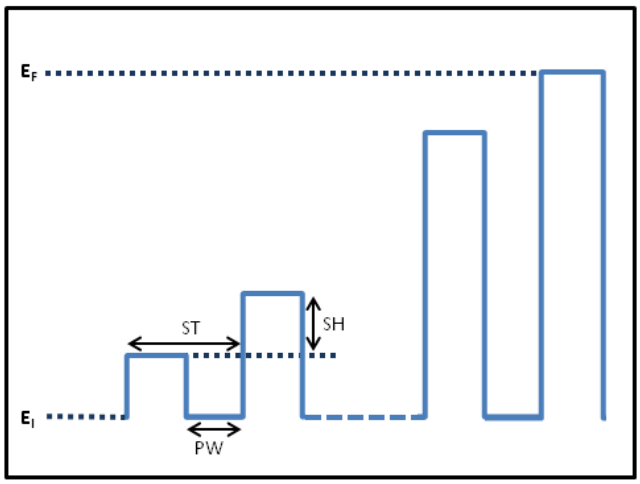

Fig. 1. Rectangular pulse shape used in the anodizing process.

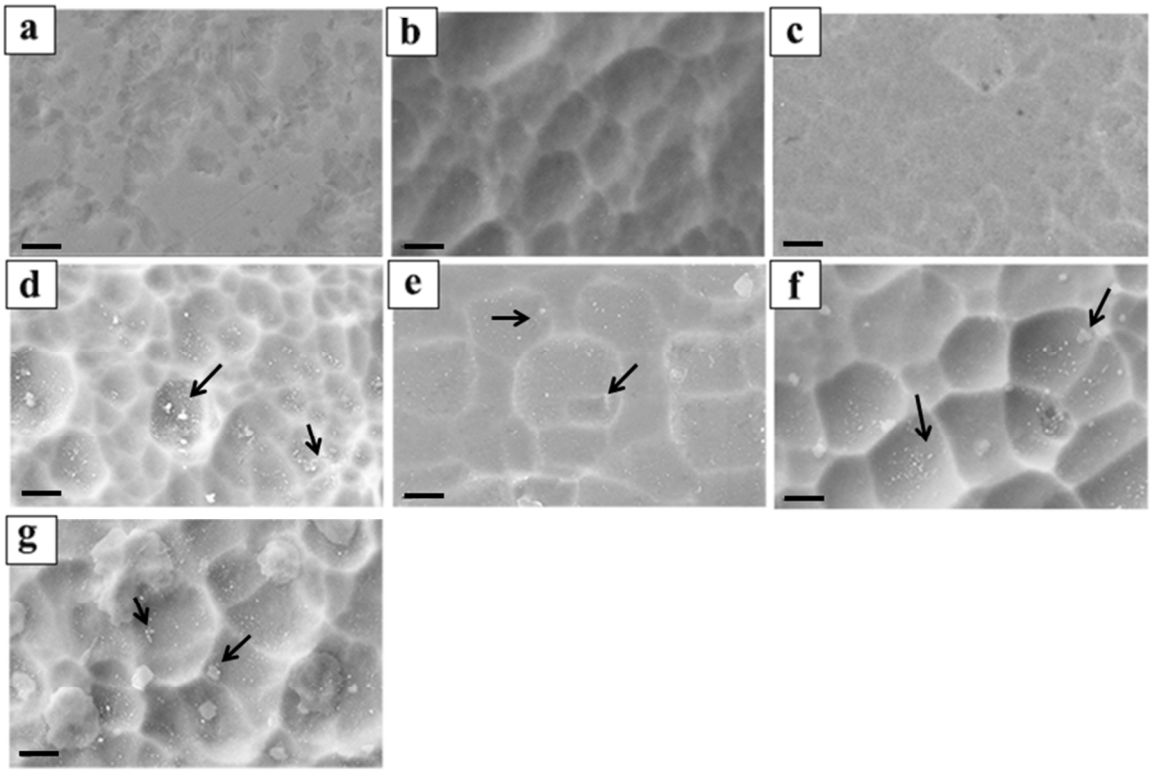

Fig. 2. SEM images of control samples: (a) Ti Treated samples, (b) NC2_200, (c) NC1_500, (d) C2_200, (e) C2_500, (f) C1_200, (g) C1_500. (Bar 5 µm).

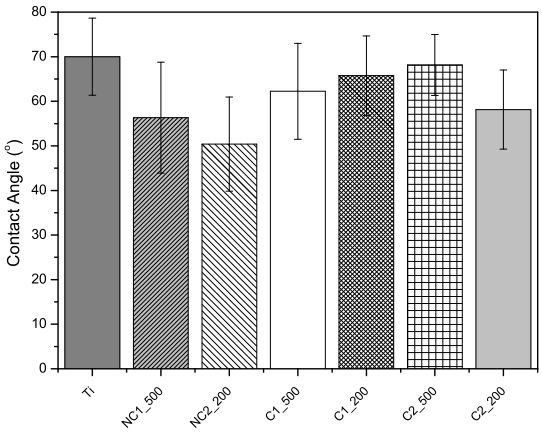

Fig. 3. Contact angle measurements [mean (standard deviation)].

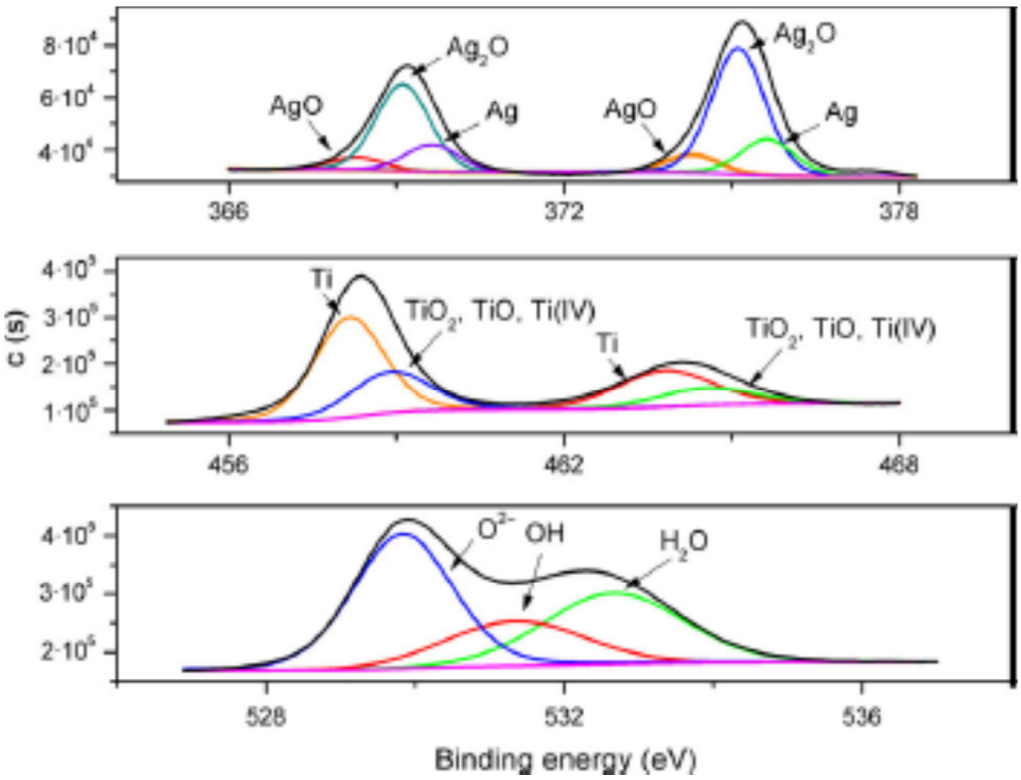

Fig. 4. Deconvoluted XPS data from sample C1_500: (a) AgO was located at highest binding energy side. (b) Ti 2p 26 was fitted to Ti subpeaks (c) O 1s consisted in 3 subpeaks. TiO2 was located at the highest binding energy side while Ti metal peak was located at the lowest binding energy side.

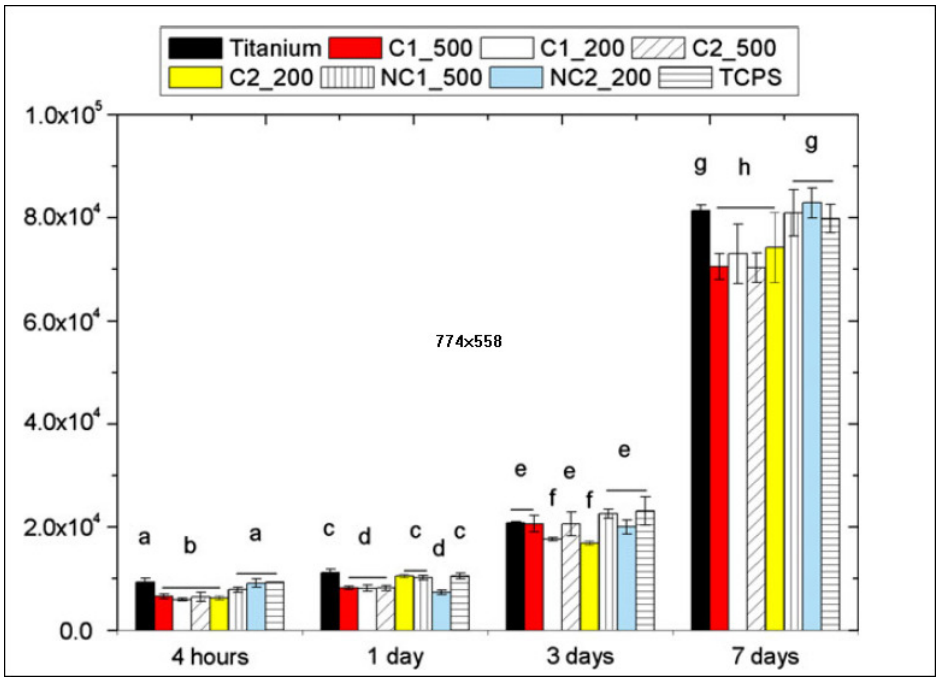

Fig. 5. Proliferation of HFFs cultured onto titanium samples with different surface treatments. The initial seeding density was 5000 cells/cm2 being the proliferation behaviors similar in all the titanium surfaces.

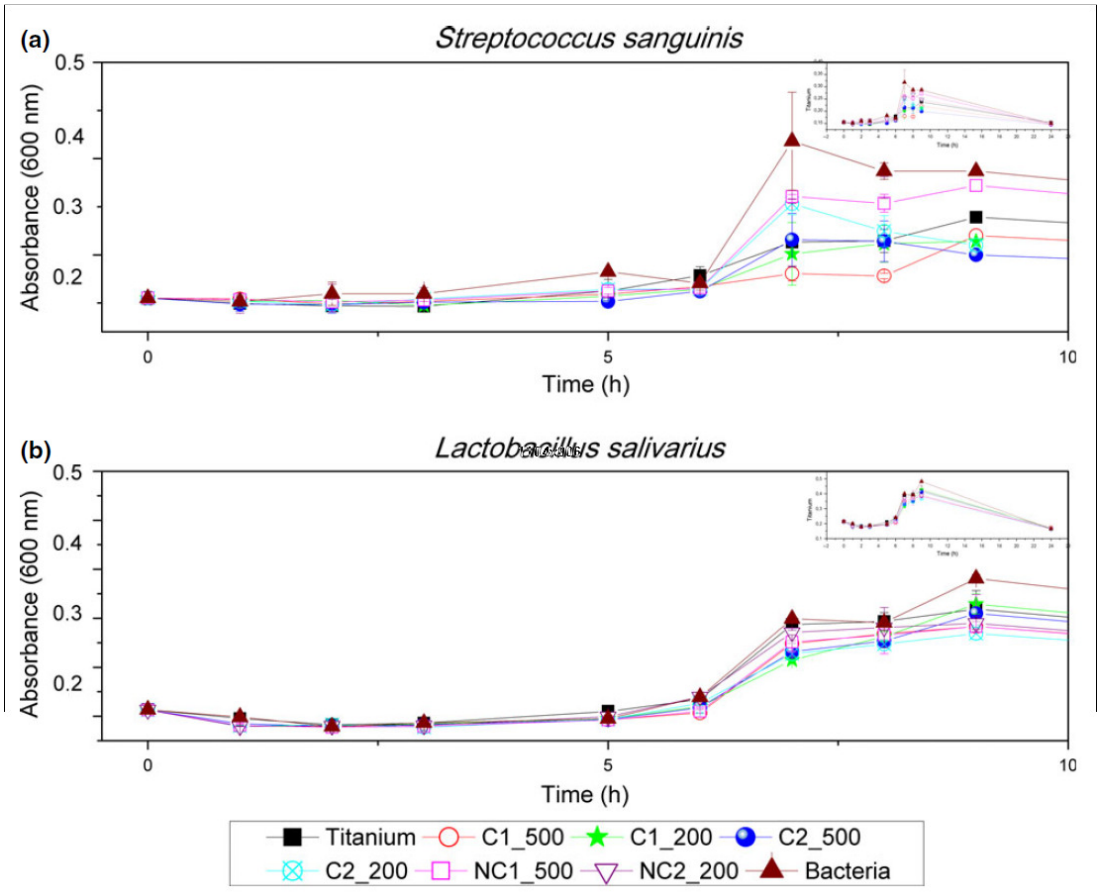

Fig. 6. Growth curve for *Lactobacillus salivarius* and *Streptococcus sanguinis*.

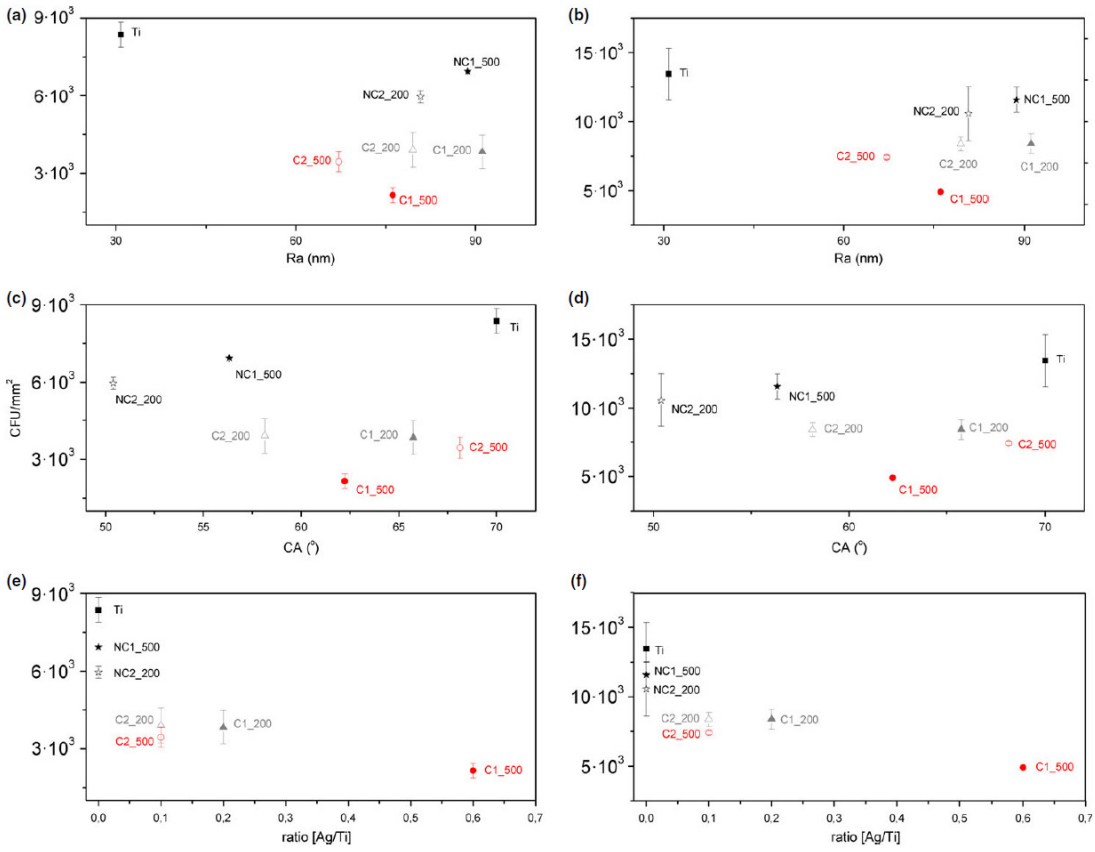

Fig 7. Bacterial adhesion to samples vs. roughness with Lactobacillus salivarius and Streptococcus sanguinis as strains. Results are displayed as CFU normalized vs. the real surface area of each sample.